The muon anomalous magnetic moment and its hadronic contributions

Massimiliano Procura

universität wien

Discoveries and Open Puzzles in Particle Physics and Gravitation,
Humboldt Kolleg, Kitzbühel, 24-28 June 2019

Outline

- The muon anomalous magnetic moment: discrepancy between SM and experiment
- Hadronic contributions: hadronic vacuum polarization and hadronic light-by-light
- Novel approach based on dispersion relations for a data-driven determination of hadronic light-by-light contribution: basic features and first numerical results
- Summary and outlook

Colangelo, Hoferichter, Procura, Stoffer, JHEP 1505 (2015), JHEP 1704 + PRL 118 (2017)

Colangelo, Hoferichter, Procura, Stoffer, JHEP 1409 (2014)

Colangelo, Hoferichter, Kubis, Procura, Stoffer, PLB 738 (2014)

Introduction

- Anomalous magnetic moments of leptons a_ℓ have played a central role in the history of particle physics by contributing to establish quantum electrodynamics

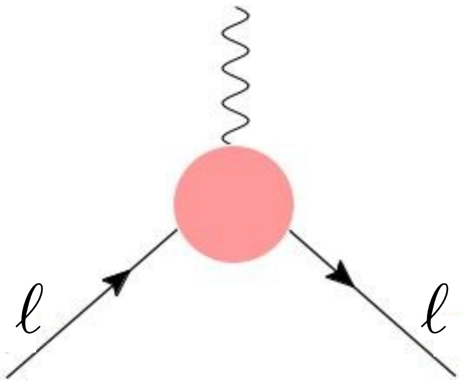

$$\vec{\mu}_\ell = g_\ell \frac{q_\ell}{2m_\ell}\vec{s} \qquad a_\ell = \frac{g_\ell - 2}{2}$$

- Dirac's relativistic theory of spin-1/2 particles predicts $g_\ell = 2$

  In the Standard Model (SM), radiative corrections are responsible for $g_\ell \neq 2$

- $a_e^{\mathrm{exp}} = 0.00115965218073(28) \;\; [0.24\ \mathrm{ppb}]$ Hanneke, Fogwell, Gabrielse (2008)

  leads to an extremely precise determination of the fine structure constant

Introduction

- The experimental world average for a_μ is dominated by the BNL E821 result

$$a_\mu^{\rm exp} = 0.00116592091(63) \;\; [0.54 \text{ ppm}]$$

Bennett et al. (2006)

$$\omega_a = \omega_{\rm spin} - \omega_{\rm cyclotron} = -a_\mu \frac{qB}{m_\mu}$$

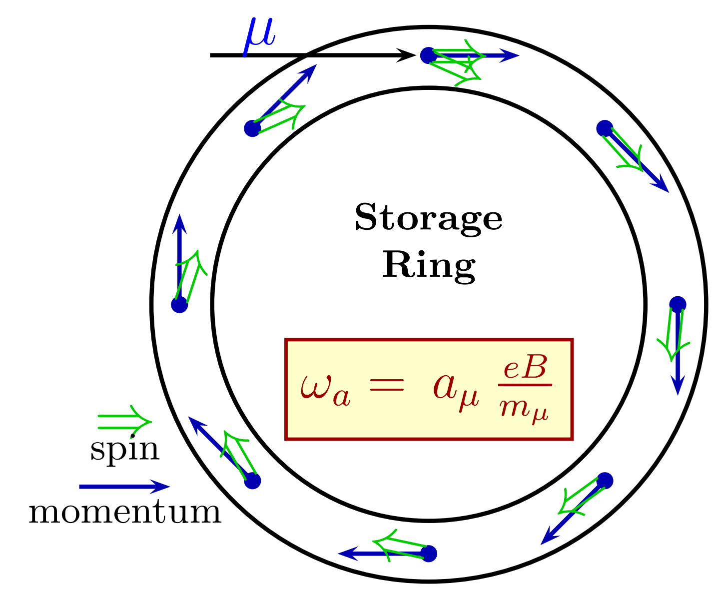

- Muon anomalous magnetic moment is particularly interesting:

  - more sensitive than a_e to weak and strong interaction effects and New Physics scales $(\Delta a_\ell \propto m_\ell^2/M^2)$

  - discrepancy $a_\mu^{\rm exp} - a_\mu^{\rm SM} \sim 3\,\sigma$: open puzzle

Introduction

The result of the BNL E821 experiment vs SM prediction

	$a_\mu \times 10^{11}$	$\Delta a_\mu \times 10^{11}$
BNL E821	116 592 091	63
QED $\mathcal{O}(\alpha)$	116 140 973.21	0.03
QED $\mathcal{O}(\alpha^2)$	413 217.63	0.01
QED $\mathcal{O}(\alpha^3)$	30 141.90	0.00
QED $\mathcal{O}(\alpha^4)$	381.01	0.02
QED $\mathcal{O}(\alpha^5)$	5.09	0.01
QED total	116 584 718.85	0.04
EW	153.6	1.0
LO HVP	6 949	43
NLO HVP	−98	1
NNLO HVP	12.4	0.1
LO HLbL	116	40
NLO HLbL	3	2
Hadronic total	6982	59
Theory total	116 591 855	59

$$a_\mu^{\mathrm{exp}} - a_\mu^{\mathrm{SM}} \sim 3\,\sigma$$

Introduction

The result of the BNL E821 experiment vs SM prediction

	$a_\mu \times 10^{11}$	$\Delta a_\mu \times 10^{11}$
BNL E821	116 592 091	63
QED $\mathcal{O}(\alpha)$	116 140 973.21	0.03
QED $\mathcal{O}(\alpha^2)$	413 217.63	0.01
QED $\mathcal{O}(\alpha^3)$	30 141.90	0.00
QED $\mathcal{O}(\alpha^4)$	381.01	0.02
QED $\mathcal{O}(\alpha^5)$	5.09	0.01
QED total	116 584 718.85	0.04
EW	153.6	1.0
LO HVP	6 949	43
NLO HVP	−98	1
NNLO HVP	12.4	0.1
LO HLbL	116	40
NLO HLbL	3	2
Hadronic total	6982	59
Theory total	116 591 855	59

$$a_\mu^{\exp} - a_\mu^{\rm SM} \sim 3\,\sigma$$

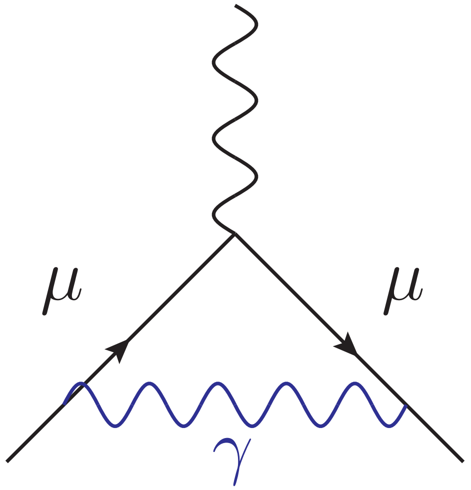

Schwinger 1948

Introduction

The result of the BNL E821 experiment vs SM prediction

	$a_\mu \times 10^{11}$	$\Delta a_\mu \times 10^{11}$
BNL E821	116 592 091	63
QED $\mathcal{O}(\alpha)$	116 140 973.21	0.03
QED $\mathcal{O}(\alpha^2)$	413 217.63	0.01
QED $\mathcal{O}(\alpha^3)$	30 141.90	0.00
QED $\mathcal{O}(\alpha^4)$	381.01	0.02
QED $\mathcal{O}(\alpha^5)$	5.09	0.01
QED total	116 584 718.85	0.04
EW	153.6	1.0
LO HVP	6 949	43
NLO HVP	−98	1
NNLO HVP	12.4	0.1
LO HLbL	116	40
NLO HLbL	3	2
Hadronic total	6982	59
Theory total	116 591 855	59

$$a_\mu^{\rm exp} - a_\mu^{\rm SM} \sim 3\,\sigma$$

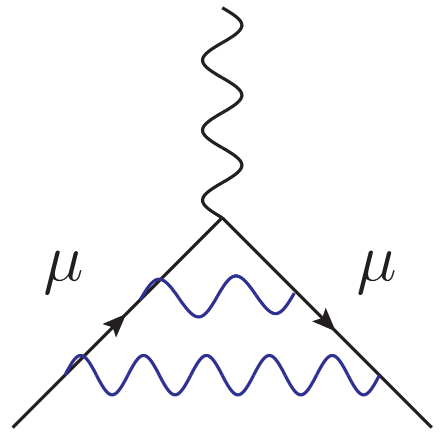

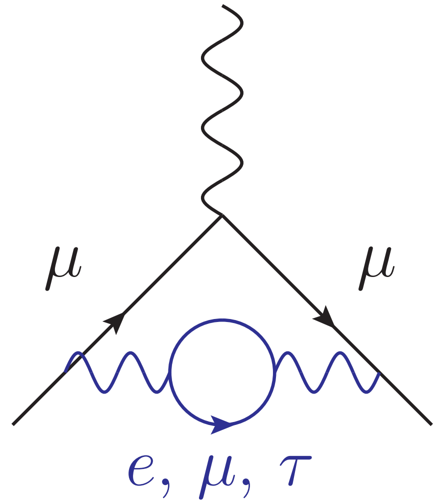

Petermann 1957
Sommerfield 1957

Introduction

The result of the BNL E821 experiment vs SM prediction

	$a_\mu \times 10^{11}$	$\Delta a_\mu \times 10^{11}$
BNL E821	116 592 091	63
QED $\mathcal{O}(\alpha)$	116 140 973.21	0.03
QED $\mathcal{O}(\alpha^2)$	413 217.63	0.01
QED $\mathcal{O}(\alpha^3)$	30 141.90	0.00
QED $\mathcal{O}(\alpha^4)$	381.01	0.02
QED $\mathcal{O}(\alpha^5)$	5.09	0.01
QED total	116 584 718.85	0.04
EW	153.6	1.0
LO HVP	6 949	43
NLO HVP	−98	1
NNLO HVP	12.4	0.1
LO HLbL	116	40
NLO HLbL	3	2
Hadronic total	6982	59
Theory total	116 591 855	59

$$a_\mu^{\mathrm{exp}} - a_\mu^{\mathrm{SM}} \sim 3\,\sigma$$

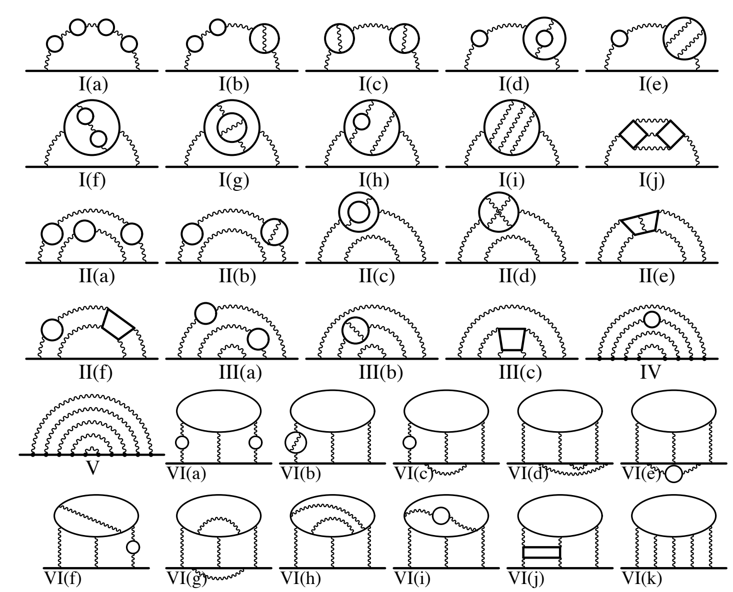

Kinoshita et al. 2012

Introduction

The result of the BNL E821 experiment vs SM prediction

	$a_\mu \times 10^{11}$	$\Delta a_\mu \times 10^{11}$
BNL E821	116 592 091	63
QED $\mathcal{O}(\alpha)$	116 140 973.21	0.03
QED $\mathcal{O}(\alpha^2)$	413 217.63	0.01
QED $\mathcal{O}(\alpha^3)$	30 141.90	0.00
QED $\mathcal{O}(\alpha^4)$	381.01	0.02
QED $\mathcal{O}(\alpha^5)$	5.09	0.01
QED total	116 584 718.85	0.04
EW	153.6	1.0
LO HVP	6 949	43
NLO HVP	−98	1
NNLO HVP	12.4	0.1
LO HLbL	116	40
NLO HLbL	3	2
Hadronic total	6982	59
Theory total	116 591 855	59

$$a_\mu^{\mathrm{exp}} - a_\mu^{\mathrm{SM}} \sim 3\,\sigma$$

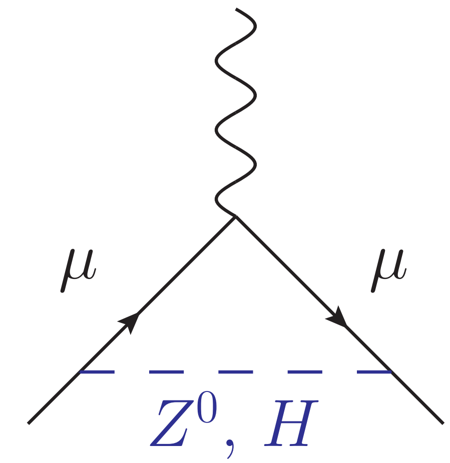

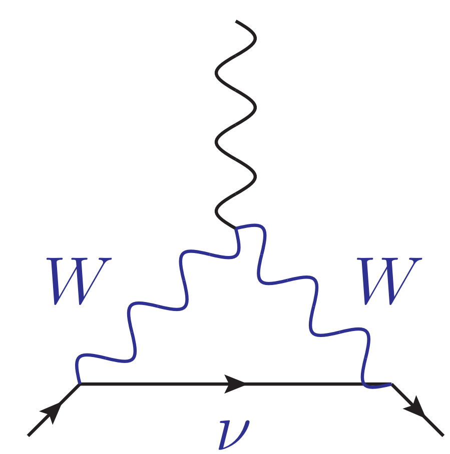

Introduction

The result of the BNL E821 experiment vs SM prediction

	$a_\mu \times 10^{11}$	$\Delta a_\mu \times 10^{11}$
BNL E821	116 592 091	63
QED $\mathcal{O}(\alpha)$	116 140 973.21	0.03
QED $\mathcal{O}(\alpha^2)$	413 217.63	0.01
QED $\mathcal{O}(\alpha^3)$	30 141.90	0.00
QED $\mathcal{O}(\alpha^4)$	381.01	0.02
QED $\mathcal{O}(\alpha^5)$	5.09	0.01
QED total	116 584 718.85	0.04
EW	153.6	1.0
LO HVP	6 949	43
NLO HVP	−98	1
NNLO HVP	12.4	0.1
LO HLbL	116	40
NLO HLbL	3	2
Hadronic total	6982	59
Theory total	116 591 855	59

$$a_\mu^{\text{exp}} - a_\mu^{\text{SM}} \sim 3\,\sigma$$

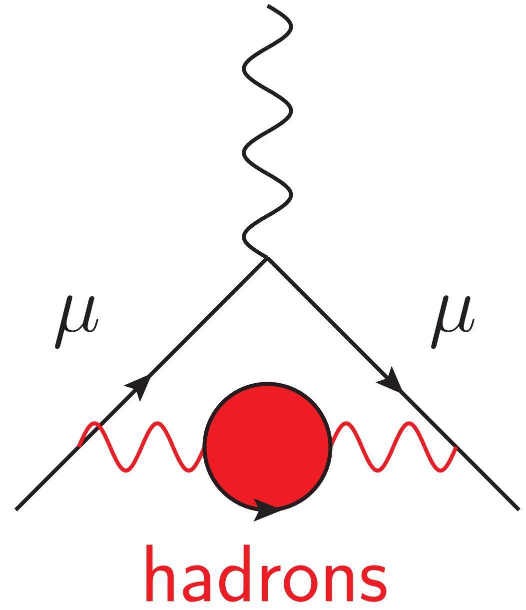

Low-energy strong interaction effects: non-perturbative!

Introduction

The result of the BNL E821 experiment vs SM prediction

	$a_\mu \times 10^{11}$	$\Delta a_\mu \times 10^{11}$
BNL E821	116 592 091	63
QED $\mathcal{O}(\alpha)$	116 140 973.21	0.03
QED $\mathcal{O}(\alpha^2)$	413 217.63	0.01
QED $\mathcal{O}(\alpha^3)$	30 141.90	0.00
QED $\mathcal{O}(\alpha^4)$	381.01	0.02
QED $\mathcal{O}(\alpha^5)$	5.09	0.01
QED total	116 584 718.85	0.04
EW	153.6	1.0
LO HVP	6 949	43
NLO HVP	−98	1
NNLO HVP	12.4	0.1
LO HLbL	116	40
NLO HLbL	3	2
Hadronic total	6982	59
Theory total	116 591 855	59

$$a_\mu^{\mathrm{exp}} - a_\mu^{\mathrm{SM}} \sim 3\,\sigma$$

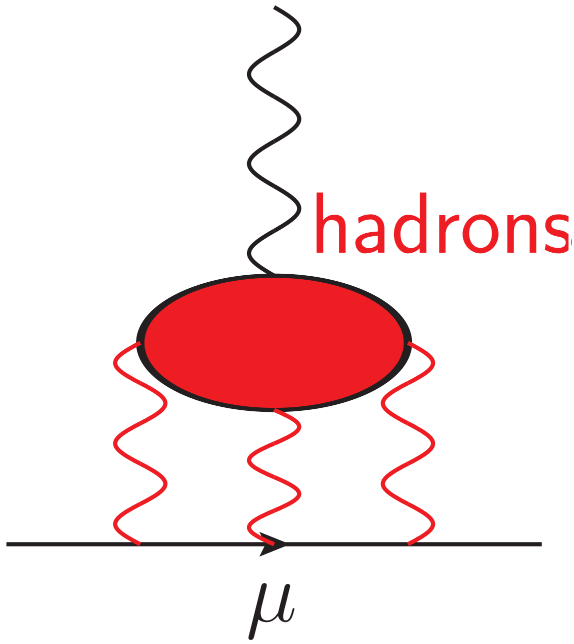

Low-energy strong interaction effects: non-perturbative!

Introduction

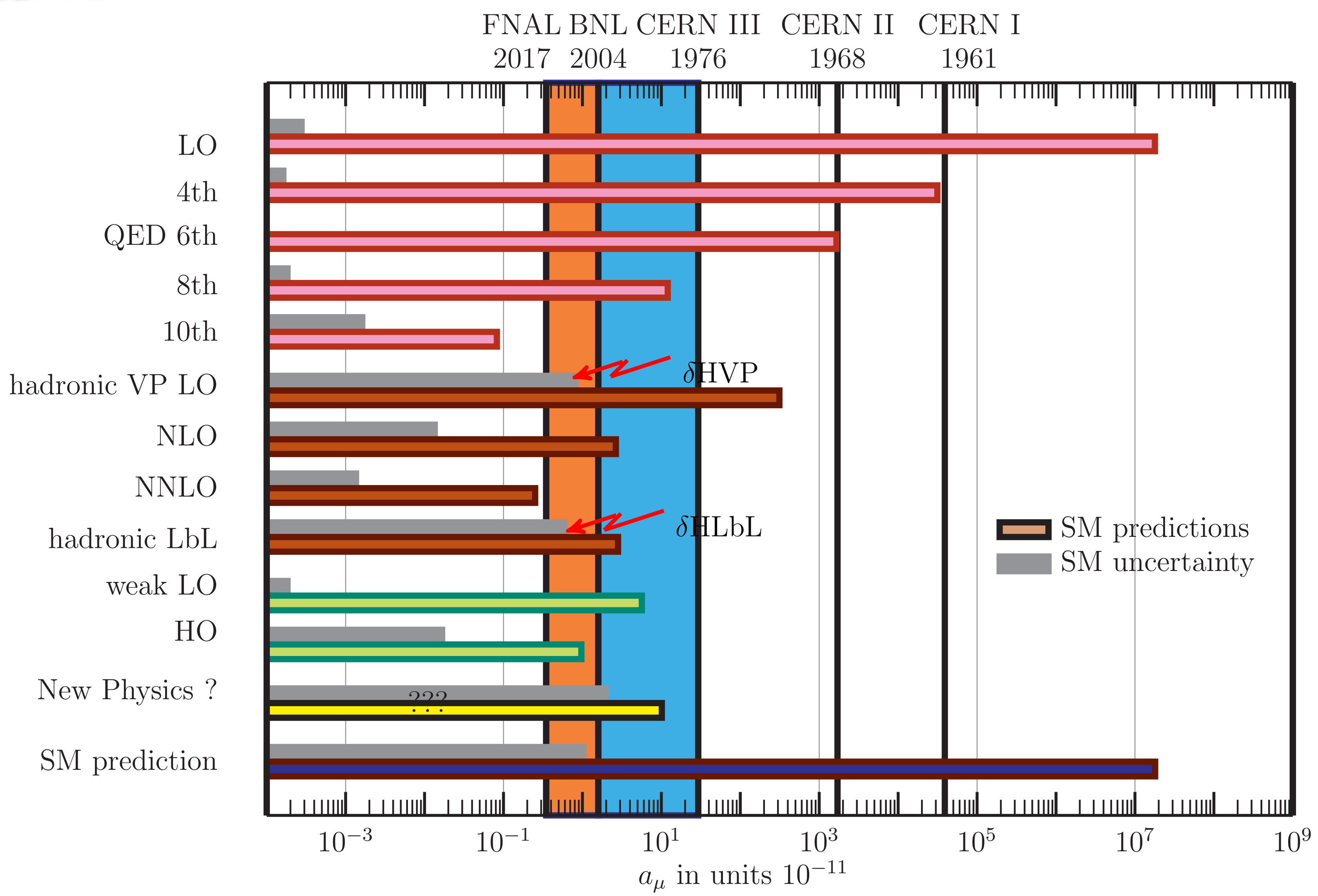

Jegerlehner (2015)

New experiment (FNAL E989) expected to improve the precision by a factor of 4

▶ crucial and timely to scrutinize SM prediction, theory uncertainties

Introduction

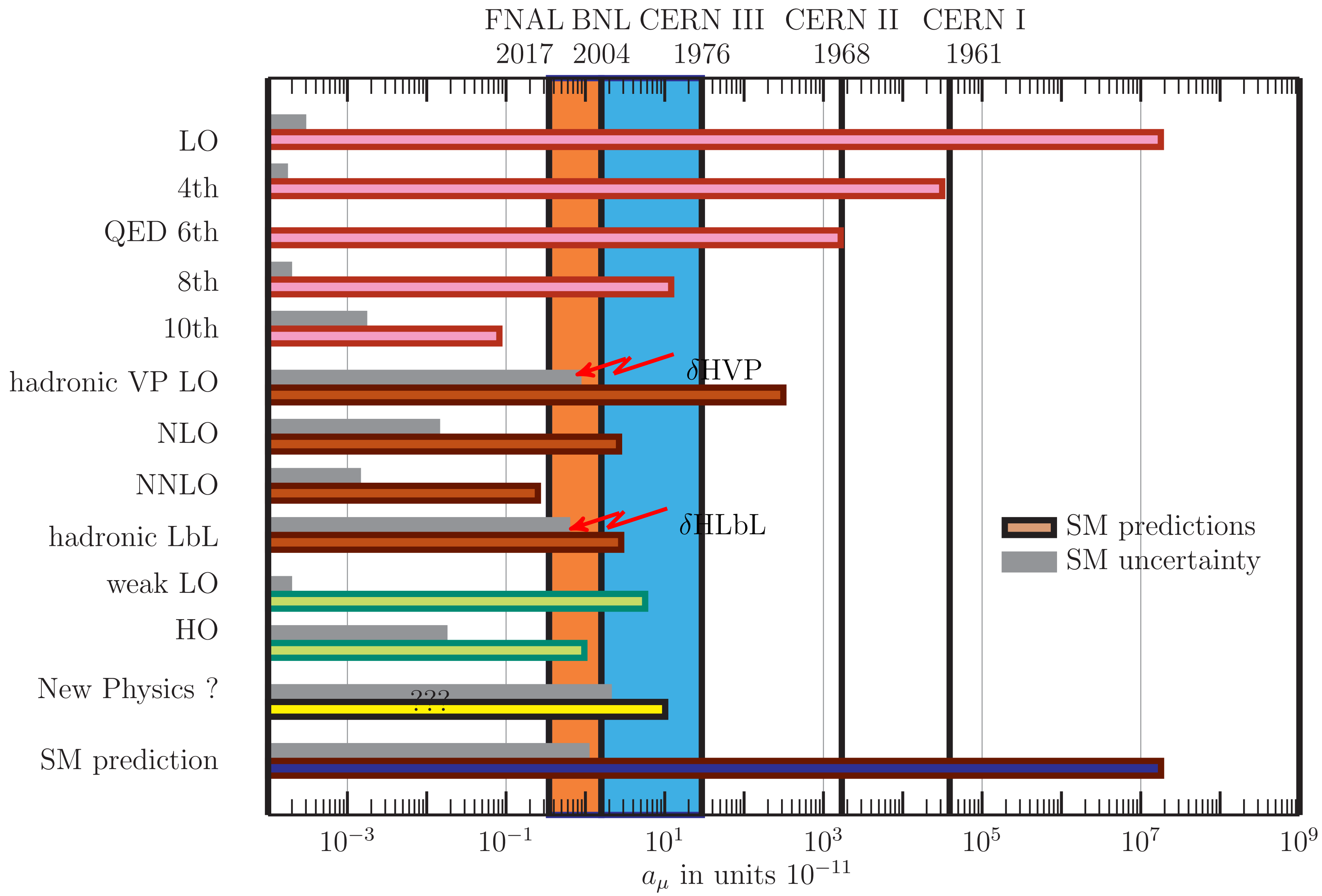

Jegerlehner (2015)

Paradigmatic example of precision experiments at the intensity frontier: look for deviations from the SM due to quantum (virtual) effects

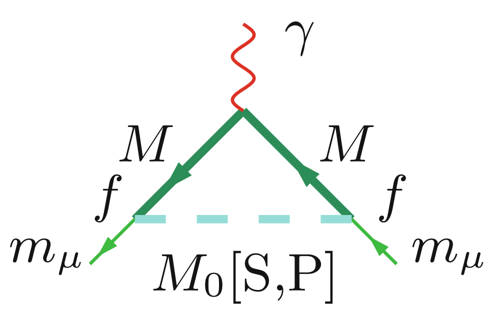

Hadronic vacuum polarization

- The crucial limiting factor in the accuracy of SM predictions for a_μ is control over hadronic contributions, responsible for most of the theory uncertainty

- The most precise determination of the LO-HVP relies on a dispersive approach:

  - Gauge invariance: $i \int d^4x \, e^{iq\cdot x} \langle 0|T\{j_\mu^{\mathrm{em}}(x) j_\nu^{\mathrm{em}}(0)\}|0\rangle = -(q^2 g_{\mu\nu} - q_\mu q_\nu)\, \Pi(q^2)$

    parameterized in terms of a single scalar function of one kinematic variable

Hadronic vacuum polarization

- The crucial limiting factor in the accuracy of SM predictions for a_μ is control over hadronic contributions, responsible for most of the theory uncertainty

- The most precise determination of the LO-HVP relies on a dispersive approach:
  - Gauge invariance: $i\int d^4x\, e^{iq\cdot x}\langle 0|T\{j_\mu^{\text{em}}(x)j_\nu^{\text{em}}(0)\}|0\rangle = -(q^2 g_{\mu\nu} - q_\mu q_\nu)\,\Pi(q^2)$
  - Analyticity: $\Pi^{\text{ren}}(q^2) = \Pi(q^2) - \Pi(0) = \frac{q^2}{4\pi}\int_{4m_\pi^2}^{\infty} ds\, \frac{\operatorname{Im}\Pi(s)}{s(s-q^2-i\epsilon)}$

  discontinuity along a branch cut corresponding to physical processes

Hadronic vacuum polarization

- The crucial limiting factor in the accuracy of SM predictions for a_μ is control over hadronic contributions, responsible for most of the theory uncertainty

- The most precise determination of the LO-HVP relies on a dispersive approach:

  - Gauge invariance: $i \int d^4x \, e^{iq\cdot x} \langle 0 | T\{ j_\mu^{\text{em}}(x) j_\nu^{\text{em}}(0) \} | 0 \rangle = -(q^2 g_{\mu\nu} - q_\mu q_\nu)\, \Pi(q^2)$

  - Analyticity: $\Pi^{\text{ren}}(q^2) = \Pi(q^2) - \Pi(0) = \dfrac{q^2}{4\pi} \displaystyle\int_{4m_\pi^2}^{\infty} ds \, \frac{\operatorname{Im}\Pi(s)}{s(s - q^2 - i\epsilon)}$

  - Unitarity (optical theorem):

Im 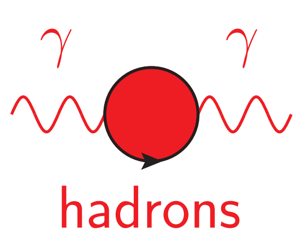

$\Leftrightarrow$ $\Big|$ 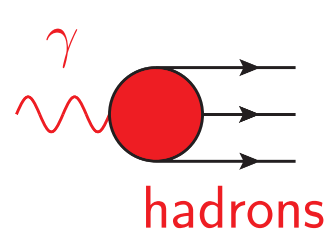

$\Big|^2$ $\propto \sigma_{\text{tot}}(e^+e^- \to \text{hadrons})$

Hadronic vacuum polarization

- The crucial limiting factor in the accuracy of SM predictions for a_μ is control over hadronic contributions, responsible for most of the theory uncertainty

- The most precise determination of the LO-HVP relies on a dispersive approach:

  - Gauge invariance: $i\int d^4x\, e^{iq\cdot x}\langle 0|T\{j_\mu^{\rm em}(x) j_\nu^{\rm em}(0)\}|0\rangle = -(q^2 g_{\mu\nu} - q_\mu q_\nu)\, \Pi(q^2)$

  - Analyticity: $\Pi^{\rm ren}(q^2) = \Pi(q^2) - \Pi(0) = \dfrac{q^2}{4\pi}\displaystyle\int_{4m_\pi^2}^\infty ds\, \frac{{\rm Im}\,\Pi(s)}{s(s-q^2-i\epsilon)}$

  - Unitarity (optical theorem):

$$
{\rm Im}\,\Pi(s) = \frac{s}{4\pi\alpha(s)}\,\sigma_{\rm tot}(e^+e^-\to \text{hadrons}) = \frac{\alpha(s)}{3}\, R^{\rm had}(s)
$$

Hadronic vacuum polarization

- The crucial limiting factor in the accuracy of SM predictions for a_μ is control over hadronic contributions, responsible for most of the theory uncertainty

- LO-HVP is obtained by integrating the hadronic R-ratio weighted with a perturbative QED kernel:

$$a_\mu^{\mathrm{LO-HVP}} = \frac{1}{3}\left(\frac{\alpha}{\pi}\right)^2 \int_{4m_\pi^2}^{\infty} \frac{ds}{s}\, K(s)\, R^{\mathrm{had}}(s)$$

dominated by the low-energy region (in particular ππ contribution)

- Dedicated e^+e^- program (Belle II, BES-III, KLOE, BaBar, SND, CMD-3, SND, KEDR) with the goal to improve the presently quoted sub-percent accuracy

Hadronic vacuum polarization

- The crucial limiting factor in the accuracy of SM predictions for a_μ is control over hadronic contributions, responsible for most of the theory uncertainty

- LO-HVP is obtained by integrating the hadronic R-ratio weighted with a perturbative QED kernel :

$$a_\mu^{\mathrm{LO-HVP}} = \frac{1}{3}\left(\frac{\alpha}{\pi}\right)^2 \int_{4m_\pi^2}^{\infty} \frac{ds}{s}\, K(s)\, R^{\mathrm{had}}(s)$$

dominated by the low-energy region (in particular ππ contribution)

- Recent world-wide efforts for a lattice QCD determination of the LO-HVP

Several collaborations (RBC/UKQCD, HPQCD/FNAL/MILC, BMW, ETM, CLS-Mainz):
physical pion mass ensembles, disconnected contributions, QED and strong isospin breaking corrections,
finite volume and continuum extrapolations. Quoted uncertainties are presently about 2 percent

Hadronic light-by-light

- Hadronic light-by-light (HLbL) is more problematic: until recently only model calculations and some high-energy and low-energy constraints

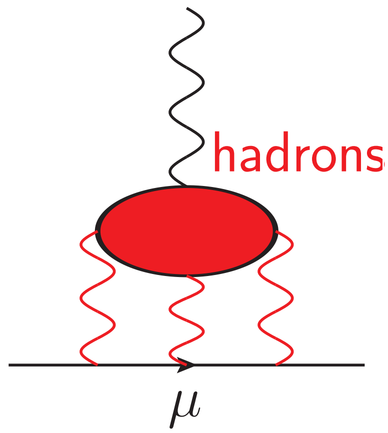

a_μ^{HLbL} in 10^{-11} units

Contribution	BPP	HKS	KN	MV	BP	PdRV	N/JN
π^0, η, η'	85±13	82.7±6.4	83±12	114±10	–	114±13	99±16
π, K loops	−19±13	−4.5±8.1	–	–	–	−19±19	−19±13
π, K loops + other subleading in N_c	–	–	–	0±10	–	–	–
axial vectors	2.5±1.0	1.7±1.7	–	22± 5	–	15±10	22± 5
scalars	−6.8±2.0	–	–	–	–	−7± 7	−7± 2
quark loops	21± 3	9.7±11.1	–	–	–	2.3	21± 3
total	83±32	89.6±15.4	80±40	136±25	110±40	105±26	116±39

Two global evaluations: Bijnens, Pallante, Prades (1995, 1996) and Hayakawa, Kinoshita, Sanda (1995, 1996)

KN = Knecht, Nyffeler; MV = Melnikov, Vainshtein; PdRV = Prades, de Rafael, Vainshtein; JN= Jegerlehner, Nyffeler

Hadronic light-by-light

- Hadronic light-by-light (HLbL) is more problematic: until recently only model calculations and some high-energy and low-energy constraints

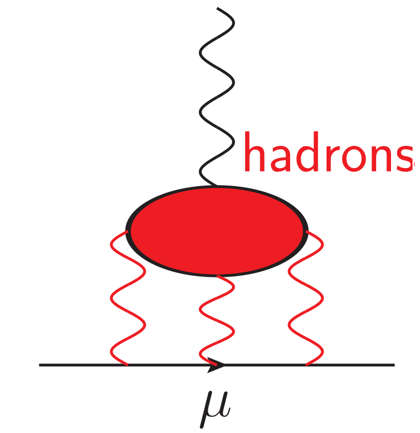

a_μ^{HLbL} in 10^{-11} units

Contribution	BPP	HKS	KN	MV	BP	PdRV	N/JN
π^0, η, η'	85±13	82.7±6.4	83±12	114±10	–	114±13	99±16
π, K loops	−19±13	−4.5±8.1	–	–	–	−19±19	−19±13
π, K loops + other subleading in N_c	–	–	–	0±10	–	–	–
axial vectors	2.5±1.0	1.7±1.7	–	22± 5	–	15±10	22± 5
scalars	−6.8±2.0	–	–	–	–	−7± 7	−7± 2
quark loops	21± 3	9.7±11.1	–	–	–	2.3	21± 3
total	83±32	89.6±15.4	80±40	136±25	110±40	105±26	116±39

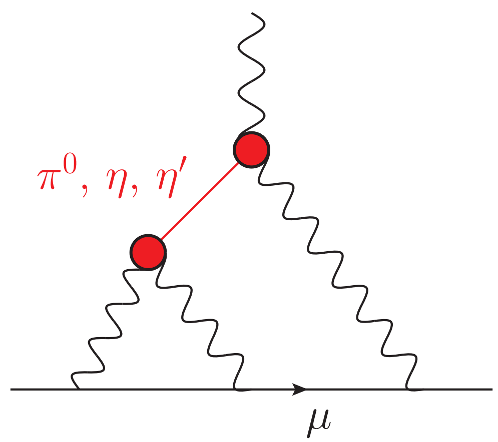

Two global evaluations: Bijnens, Pallante, Prades (1995, 1996) and Hayakawa, Kinoshita, Sanda (1995, 1996)

KN = Knecht, Nyffeler; MV = Melnikov, Vainshtein; PdRV = Prades, de Rafael, Vainshtein; JN= Jegerlehner, Nyffeler

Hadronic light-by-light

- Hadronic light-by-light (HLbL) is more problematic: until recently only model calculations and some high-energy and low-energy constraints

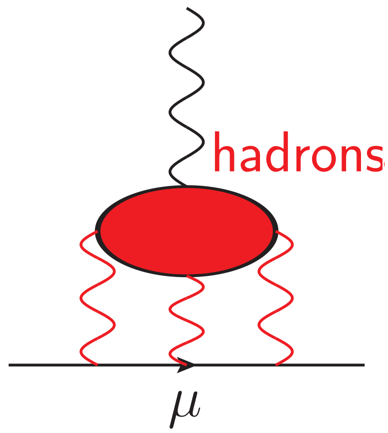

a_μ^{HLbL} in 10^{-11} units

Contribution	BPP	HKS	KN	MV	BP	PdRV	N/JN
π^0, η, η'	85±13	82.7±6.4	83±12	114±10	–	114±13	99±16
π, K loops	−19±13	−4.5±8.1	–	–	–	−19±19	−19±13
π, K loops + other subleading in N_c	–	–	–	0±10	–	–	–
axial vectors	2.5±1.0	1.7±1.7	–	22± 5	–	15±10	22± 5
scalars	−6.8±2.0	–	–	–	–	−7± 7	−7± 2
quark loops	21± 3	9.7±11.1	–	–	–	2.3	21± 3
total	83±32	89.6±15.4	80±40	136±25	110±40	105±26	116±39

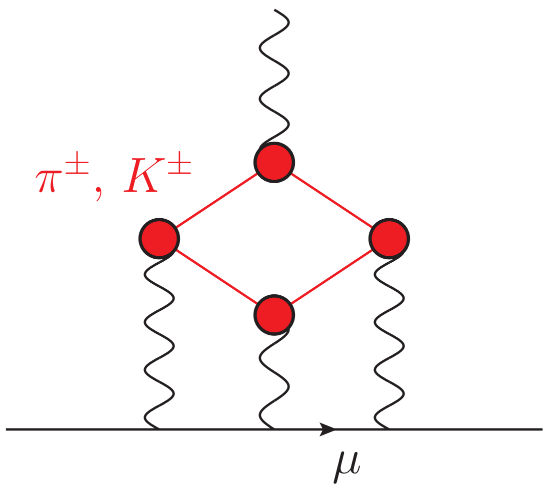

Two global evaluations: Bijnens, Pallante, Prades (1995, 1996) and Hayakawa, Kinoshita, Sanda (1995, 1996)

KN = Knecht, Nyffeler; MV = Melnikov, Vainshtein; PdRV = Prades, de Rafael, Vainshtein; JN= Jegerlehner, Nyffeler

Hadronic light-by-light

- Hadronic light-by-light (HLbL) is more problematic: until recently only model calculations and some high-energy and low-energy constraints

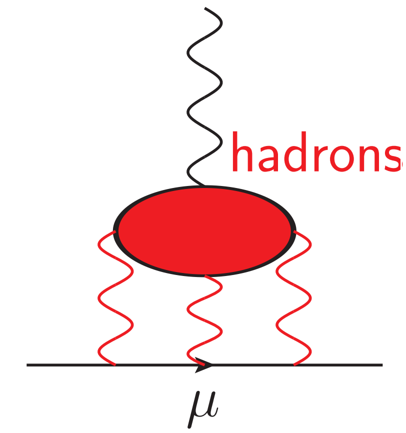

a_μ^{HLbL} in 10^{-11} units

Contribution	BPP	HKS	KN	MV	BP	PdRV	N/JN
π^0, η, η'	85±13	82.7±6.4	83±12	114±10	–	114±13	99±16
π, K loops	−19±13	−4.5±8.1	–	–	–	−19±19	−19±13
π, K loops + other subleading in N_c	–	–	–	0±10	–	–	–
axial vectors	2.5±1.0	1.7±1.7	–	22± 5	–	15±10	22± 5
scalars	−6.8±2.0	–	–	–	–	−7± 7	−7± 2
quark loops	21± 3	9.7±11.1	–	–	–	2.3	21± 3
total	83±32	89.6±15.4	80±40	136±25	110±40	105±26	116±39

Jegerlehner (2015)

≈ 8±3

102±39

The two most often quoted estimates: Prades, de Rafael, Vainshtein (2009) and Jegerlehner, Nyffeler (2009)

Hadronic light-by-light

- Hadronic light-by-light (HLbL) is more problematic: until recently only model calculations and some high-energy and low-energy constraints

  Quoted uncertainties are guesstimates!

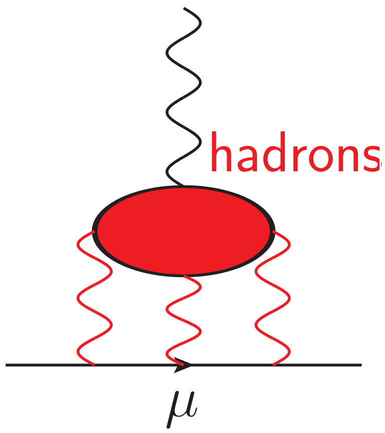

  ▶ a reliable uncertainty estimate for HLbL is still an open issue

- How to reduce model dependence? Recent strategies for an improved determination:

  ▶ lattice QCD: first computations at physical pion masses with leading disconnected contributions performed (with large systematic errors due to finite volume and finite lattice spacing) RBC/UKQCD (Blum et al., 2015-2017)
  Mainz lattice group: pion-pole contribution (Gerardin, Meyer, Nyffeler, 2019)

  ▶ dispersion theory to make the evaluation as data-driven as possible

Dispersive approach to HLbL

- Exploits fundamental principles:
  - gauge invariance and crossing symmetry
  - unitarity and analyticity

  to relate HLbL to experimentally accessible quantities

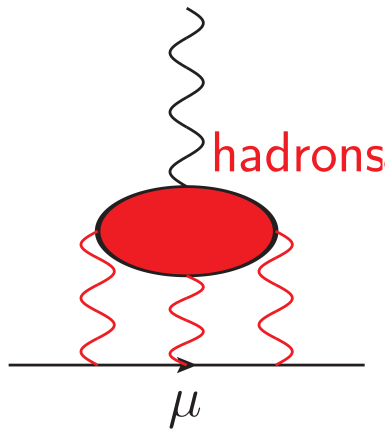

- Much more challenging task than for the hadronic vacuum polarization due to the complexity of the HLbL tensor, which is the key object of our analysis

- Defines and relates single contributions to HLbL to form factors and cross sections

Colangelo, Hoferichter, Procura, Stoffer, JHEP 1505 (2015), JHEP 1704 + PRL 118 (2017)

Colangelo, Hoferichter, Procura, Stoffer, JHEP 1409 (2014)

Colangelo, Hoferichter, Kubis, Procura, Stoffer, PLB 738 (2014)

HLbL tensor and master formula

$$\Pi^{\mu\nu\lambda\sigma}(q_1,q_2,q_3) = -i\int d^4x\, d^4y\, d^4z\, e^{-i(q_1\cdot x+q_2\cdot y+q_3\cdot z)}\langle 0|T\{j^\mu_{\rm em}(x)j^\nu_{\rm em}(y)j^\lambda_{\rm em}(z)j^\sigma_{\rm em}(0)\}|0\rangle$$

- Lorentz covariance: 138 structures that are redundant due to Ward identities
- Derived 54 generating Lorentz structures that are manifestly gauge invariant and crossing symmetric. The scalar functions Π_i are free of kinematic singularities and zeros: their analytic structure is dictated by dynamics only

$$\Pi^{\mu\nu\lambda\sigma}(q_1,q_2,q_3) = \sum_{i=1}^{54} T_i^{\mu\nu\lambda\sigma}\Pi_i(s,t,u;q_j^2)$$

- Obtained a general master formula:

$$a_\mu^{\rm HLbL} = \frac{2\alpha^3}{3\pi^2}\int_0^\infty dQ_1\int_0^\infty dQ_2\int_{-1}^1 d\tau\sqrt{1-\tau^2}\,Q_1^3\,Q_2^3\sum_{i=1}^{12}T_i(Q_1,Q_2,\tau)\,\bar{\Pi}_i(Q_1,Q_2,\tau)$$

Contributions to a_μ^{HLbL}

- Unitarity in direct and crossed channel (poles and branch cuts)

$$\Pi_i^t(s,t,u) = c_i^t + \frac{\rho_{i;s}^t}{s-M_\pi^2} + \frac{\rho_{i;u}^t}{u-M_\pi^2} + \frac{1}{\pi}\int_{4M_\pi^2}^{\infty} ds' \frac{\mathrm{Im}_s \Pi_i^t(s',t,u')}{s'-s} + \frac{1}{\pi}\int_{4M_\pi^2}^{\infty} du' \frac{\mathrm{Im}_u \Pi_i^t(s',t,u')}{u'-u}$$

- The lightest intermediate states dominate (in agreement with models)

- HLbL tensor can be split up into contributions with different topologies:

$$\Pi_{\mu\nu\lambda\sigma} = \Pi_{\mu\nu\lambda\sigma}^{\pi^0\text{-pole}} + \Pi_{\mu\nu\lambda\sigma}^{\text{box}} + \bar{\Pi}_{\mu\nu\lambda\sigma} + \ldots$$

one-pion intermediate state :

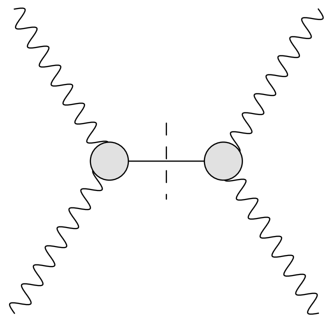

Contributions to a_μ^{HLbL}

- Unitarity in direct and crossed channel (poles and branch cuts)

$$\Pi_i^t(s,t,u) = c_i^t + \frac{\rho_{i;s}^t}{s-M_\pi^2} + \frac{\rho_{i;u}^t}{u-M_\pi^2} + \frac{1}{\pi}\int_{4M_\pi^2}^\infty ds' \frac{\mathrm{Im}_s \Pi_i^t(s',t,u')}{s'-s} + \frac{1}{\pi}\int_{4M_\pi^2}^\infty du' \frac{\mathrm{Im}_u \Pi_i^t(s',t,u')}{u'-u}$$

- The lightest intermediate states dominate (in agreement with models)

- HLbL tensor can be split up into contributions with different topologies:

$$\Pi_{\mu\nu\lambda\sigma} = \Pi_{\mu\nu\lambda\sigma}^{\pi^0\text{-pole}} + \Pi_{\mu\nu\lambda\sigma}^{\text{box}} + \bar{\Pi}_{\mu\nu\lambda\sigma} + \dots$$

two-pion intermediate state in both channels :

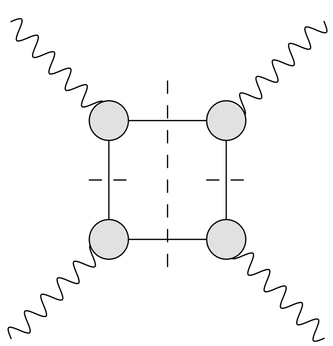

Contributions to a_μ^{HLbL}

- Unitarity in direct and crossed channel (poles and branch cuts)

$$\Pi_i^t(s,t,u) = c_i^t + \frac{\rho_{i;s}^t}{s - M_\pi^2} + \frac{\rho_{i;u}^t}{u - M_\pi^2} + \frac{1}{\pi}\int_{4M_\pi^2}^\infty ds' \frac{\mathrm{Im}_s \Pi_i^t(s',t,u')}{s'-s} + \frac{1}{\pi}\int_{4M_\pi^2}^\infty du' \frac{\mathrm{Im}_u \Pi_i^t(s',t,u')}{u'-u}$$

- The lightest intermediate states dominate (in agreement with models)

- HLbL tensor can be split up into contributions with different topologies:

$$\Pi_{\mu\nu\lambda\sigma} = \Pi_{\mu\nu\lambda\sigma}^{\pi^0\text{-pole}} + \Pi_{\mu\nu\lambda\sigma}^{\text{box}} + \bar{\Pi}_{\mu\nu\lambda\sigma} + \dots$$

two-pion state only in the direct channel:

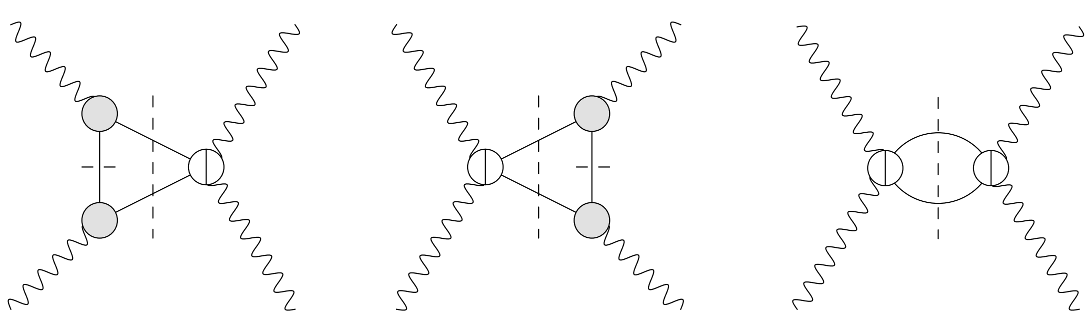

Contributions to a_μ^{HLbL}

- Unitarity in direct and crossed channel (poles and branch cuts)

$$\Pi_i^t(s,t,u) = c_i^t + \frac{\rho_{i;s}^t}{s-M_\pi^2} + \frac{\rho_{i;u}^t}{u-M_\pi^2} + \frac{1}{\pi}\int_{4M_\pi^2}^\infty ds' \frac{\mathrm{Im}_s \Pi_i^t(s',t,u')}{s'-s} + \frac{1}{\pi}\int_{4M_\pi^2}^\infty du' \frac{\mathrm{Im}_u \Pi_i^t(s',t,u')}{u'-u}$$

- The lightest intermediate states dominate (in agreement with models)

- HLbL tensor can be split up into contributions with different topologies:

$$\Pi_{\mu\nu\lambda\sigma} = \Pi_{\mu\nu\lambda\sigma}^{\pi^0\text{-pole}} + \Pi_{\mu\nu\lambda\sigma}^{\text{box}} + \bar{\Pi}_{\mu\nu\lambda\sigma} + \dots$$

higher intermediate states: ongoing work

Numerical results for dispersive a_μ^{HLbL}

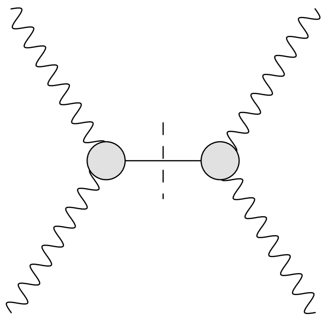

Info on pion transition form factor: $a_\mu^{\pi^0-\text{pole}} = 62.6^{+3.0}_{-2.5} \times 10^{-11}$

Hoferichter, Hoid, Kubis, Leupold, Schneider (2018)

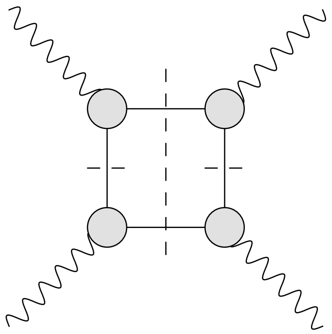

Info on pion vector form factor: $a_\mu^{\pi-\text{box}} = -15.9(2) \times 10^{-11}$

Colangelo, Hoferichter, MP, Stoffer (2017)

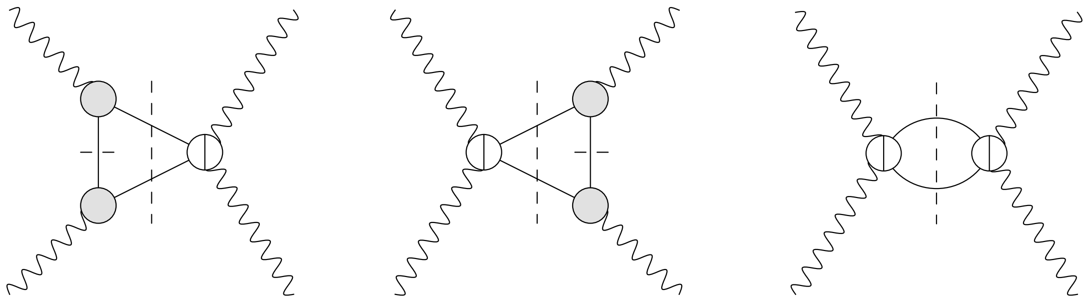

Info on helicity partial waves for $\gamma^*\gamma^* \to \pi\pi$ with S-wave $\pi\pi$ rescattering effects:

$$a_{\mu,J=0}^{\pi\pi} = -8(1) \times 10^{-11}$$

A more precise, data-driven SM evaluation of HLbL is feasible!

Outlook for dispersive a_μ^{HLbL}

Ongoing and future work:

- rescattering contributions for higher partial waves to account for prominent features in the cross sections for photon-photon to two mesons
- contributions from higher intermediate states
- systematic study of all short-distance constraints on HLbL

Will lead to a more precise SM evaluation of the muon g-2: timely!

Summary and outlook

- The discrepancy between SM prediction and experimental determination of the muon anomalous magnetic moment is an open puzzle: new physics?

- Theoretical uncertainties are dominated by hadronic contributions

- Hadronic vacuum polarization can be accurately determined using a data-driven approach based on dispersion relations
  Ongoing work: improved experimental input, better understanding of role of correlated uncertainties and systematic errors.
  Alternative determinations: lattice QCD, MUonE experiment (see talk by A. Primo)

- For the hadronic light-by-light contribution, a data-driven dispersive approach with reliable uncertainties is feasible.
  Ongoing work: refined analysis of two-meson intermediate states, study of higher intermediate states and asymptotic constraints from OPE and perturbative QCD.
  Complementary information from lattice QCD

Additional slides

A roadmap for HLbL

Colangelo, Hoferichter, Kubis, MP, Stoffer (2014)

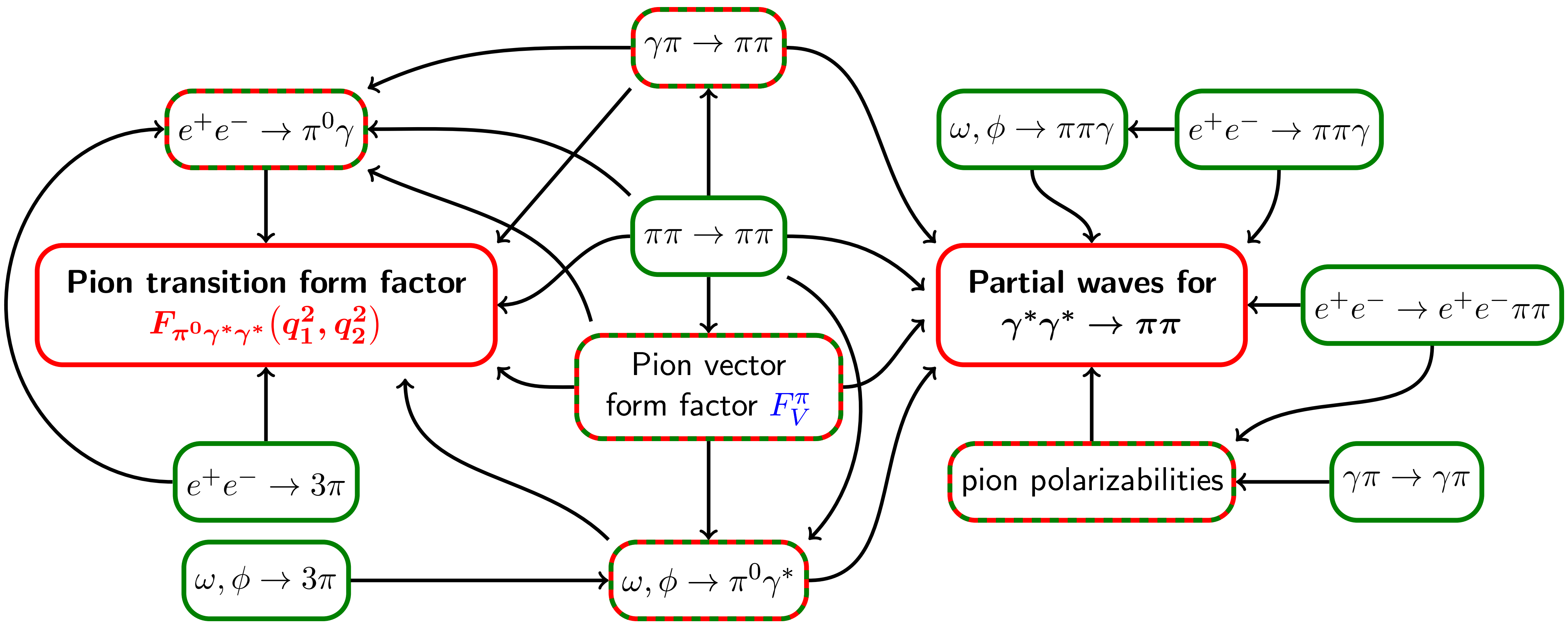

Artwork by M. Hoferichter

The HLbL tensor

- The fully off-shell HLbL tensor :

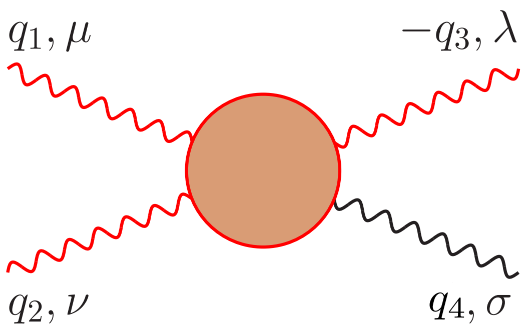

$$\Pi^{\mu\nu\lambda\sigma}(q_1, q_2, q_3) = -i \int d^4x\, d^4y\, d^4z\, e^{-i(q_1\cdot x + q_2\cdot y + q_3\cdot z)} \langle 0|T\{j^\mu_{\rm em}(x) j^\nu_{\rm em}(y) j^\lambda_{\rm em}(z) j^\sigma_{\rm em}(0)\}|0\rangle$$

- Mandelstam variables:

$$s = (q_1 + q_2)^2,\ t = (q_1 + q_3)^2,\ u = (q_2 + q_3)^2$$

- In order to extract $a_\mu^{\rm HLbL}$, $q_4 \to 0$ afterwards

Lorentz structure of HLbL tensor

- Based on Lorentz covariance the HLbL tensor can be decomposed in 138 structures

$$
\begin{aligned}
\Pi^{\mu\nu\lambda\sigma} &= g^{\mu\nu} g^{\lambda\sigma}\,\Pi^1 + g^{\mu\lambda} g^{\nu\sigma}\,\Pi^2 + g^{\mu\sigma} g^{\nu\lambda}\,\Pi^3 \\
&\quad + \sum_{\substack{k=1,2,4\\ l=1,2,3}} g^{\mu\nu} q_k^\lambda q_l^\sigma\,\Pi^4_{kl} + \sum_{\substack{j=1,3,4\\ l=1,2,3}} g^{\mu\lambda} q_j^\nu q_l^\sigma\,\Pi^5_{jl} + \sum_{\substack{j=1,3,4\\ k=1,2,4}} g^{\mu\sigma} q_j^\nu q_k^\lambda\,\Pi^6_{jk} \\
&\quad + \sum_{\substack{i=2,3,4\\ l=1,2,3}} g^{\nu\lambda} q_i^\mu q_l^\sigma\,\Pi^7_{il} + \sum_{\substack{i=2,3,4\\ k=1,2,4}} g^{\nu\sigma} q_i^\mu q_k^\lambda\,\Pi^8_{ik} + \sum_{\substack{i=2,3,4\\ j=1,3,4}} g^{\lambda\sigma} q_i^\mu q_j^\nu\,\Pi^9_{ij} \\
&\quad + \sum_{\substack{i=2,3,4\\ j=1,3,4}} \sum_{\substack{k=1,2,4\\ l=1,2,3}} q_i^\mu q_j^\nu q_k^\lambda q_l^\sigma\,\Pi^{10}_{ijkl}
\end{aligned}
$$

- In 4 space-time dimensions there are 2 linear relations among these 138 structures

Eichmann, Fischer, Heupel, Williams (2014)

- Scalar functions encode the hadronic dynamics and depend on 6 kinematic variables

- This set of functions is hugely redundant: Ward identities imply 95 linear relations among these scalar functions (kinematic zeros)

Lorentz structure of HLbL tensor

- Following Bardeen and Tung (1968) - "BT"- we contracted the HLBL tensor with

$$I_{12}^{\mu\nu} = g^{\mu\nu} - \frac{q_2^\mu q_1^\nu}{q_1 \cdot q_2}, \quad I_{34}^{\lambda\sigma} = g^{\lambda\sigma} - \frac{q_4^\lambda q_3^\sigma}{q_3 \cdot q_4}$$

  - 95 structures project to zero

- $1/q_1 \cdot q_2$ and $1/q_3 \cdot q_4$ poles eliminated by taking linear combinations of structures

- This procedure introduces kinematic singularities in the scalar functions: degeneracies in these BT Lorentz structures, e.g. as $q_1 \cdot q_2 \to 0$, $q_3 \cdot q_4 \to 0$

$$\sum_k c_k^i T_k^{\mu\nu\lambda\sigma} = q_1 \cdot q_2 X_i^{\mu\nu\lambda\sigma} + q_3 \cdot q_4 Y_i^{\mu\nu\lambda\sigma}$$

Lorentz structure of HLbL tensor

- Following Tarrach (1975) we extended BT set to incorporate $X_i^{\mu\nu\lambda\sigma}$, $Y_i^{\mu\nu\lambda\sigma}$ to obtain a ("BTT") generating set of structures even for $q_1 \cdot q_2 \to 0,\, q_3 \cdot q_4 \to 0$

$$\boxed{\Pi^{\mu\nu\lambda\sigma}(q_1, q_2, q_3) = \sum_{i=1}^{54} T_i^{\mu\nu\lambda\sigma} \Pi_i(s, t, u; q_j^2)}$$

- Lorentz structures are manifestly gauge invariant

- crossing symmetry is manifest (only 7 genuinely different structures, the remaining ones being obtained by crossing)

- the BTT scalar functions are free of kinematic singularities and zeros: their analytic structure is dictated by dynamics only. This makes them suitable for a dispersive treatment

Master formula for a_μ^{HLbL}

- From $\Pi_{\mu\nu\lambda\sigma}$ to a_μ^{HLbL} :

  By expanding the photon-muon vertex function around $q_4 = 0$,

$$a_\mu^{\mathrm{HLbL}} = -\frac{1}{48 m_\mu} \mathrm{Tr}\left((\not{p} + m_\mu)[\gamma^\rho, \gamma^\sigma](\not{p} + m_\mu) \Gamma_{\rho\sigma}^{\mathrm{HLbL}}(p) \right)$$

Aldin, Brodsky, Dufner, Kinoshita (1970)

where $p^2 = m_\mu^2$ and

$$\Gamma_{\rho\sigma}^{\mathrm{HLbL}}(p) = e^6 \int \frac{d^4 q_1}{(2\pi)^4} \frac{d^4 q_2}{(2\pi)^4} \gamma^\mu \frac{(\not{p} + \not{q}_1 + m_\mu)}{(p+q_1)^2 - m_\mu^2} \gamma^\lambda \frac{(\not{p} - \not{q}_2 + m_\mu)}{(p-q_2)^2 - m_\mu^2} \gamma^\nu \\ \times \frac{1}{q_1^2 q_2^2 (q_1 + q_2)^2} \frac{\partial}{\partial q_4^\rho} \Pi_{\mu\nu\lambda\sigma}(q_1, q_2, q_4 - q_1 - q_2) \Big|_{q_4 = 0}$$

Master formula for a_μ^{HLbL}

- From $\Pi_{\mu\nu\lambda\sigma}$ to a_μ^{HLbL} :

  By expanding the photon-muon vertex function around $q_4 = 0$,

$$a_\mu^{\mathrm{HLbL}} = -\frac{1}{48 m_\mu} \mathrm{Tr}\left((\not{p} + m_\mu)[\gamma^\rho, \gamma^\sigma](\not{p} + m_\mu)\Gamma_{\rho\sigma}^{\mathrm{HLbL}}(p) \right)$$

- Since there are no kinematic singularities in the BTT scalar functions, the limit $q_4 \to 0$ can be taken explicitly

$$\begin{aligned} a_\mu^{\mathrm{HLbL}} = &-\frac{e^6}{48 m_\mu} \int \frac{d^4 q_1}{(2\pi)^4} \frac{d^4 q_2}{(2\pi)^4} \frac{1}{q_1^2 q_2^2 (q_1+q_2)^2} \frac{1}{(p+q_1)^2 - m_\mu^2} \frac{1}{(p-q_2)^2 - m_\mu^2} \\ &\times \mathrm{Tr}\left((\not{p} + m_\mu)[\gamma^\rho, \gamma^\sigma](\not{p} + m_\mu)\gamma^\mu(\not{p} + \not{q}_1 + m_\mu)\gamma^\lambda(\not{p} - \not{q}_2 + m_\mu)\gamma^\nu \right) \\ &\times \sum_{i=1}^{54} \left(\frac{\partial}{\partial q_4^\rho} T^i_{\mu\nu\lambda\sigma}(q_1, q_2, q_4 - q_1 - q_2) \right) \Bigg|_{q_4=0} \Pi_i(q_1, q_2, -q_1 - q_2) \end{aligned}$$

Master formula for a_μ^{HLbL}

- We obtained a general master formula

$$a_\mu^{\text{HLbL}} = \frac{2\alpha^3}{3\pi^2}\int_0^\infty dQ_1 \int_0^\infty dQ_2 \int_{-1}^{1} d\tau \sqrt{1-\tau^2}\,Q_1^3 Q_2^3 \sum_{i=1}^{12} T_i(Q_1, Q_2, \tau)\bar{\Pi}_i(Q_1, Q_2, \tau)$$

- $Q_i^2 = -q_i^2$ are Euclidean momenta and $Q_1 \cdot Q_2 = Q_1\, Q_2\, \tau$: space-like kinematics

- Generalization of the formula for the pion pole by Knecht and Nyffeler (2002)

- We determined the integration kernels T_i .
  The scalar functions $\bar{\Pi}_i$ are linear combinations of the BTT Π_i

- Our goal: dispersive representation of HLbL scalar functions at fixed photon virtualities to be evaluated at the reduced kinematics in the master formula,

$$s = -Q_3^2 = -Q_1^2 - 2Q_1Q_2\tau - Q_2^2, \quad t = -Q_2^2, \quad u = -Q_1^2,$$
$$q_1^2 = -Q_1^2, \quad q_2^2 = -Q_2^2, \quad q_3^2 = -Q_3^2 = -Q_1^2 - 2Q_1Q_2\tau - Q_2^2, \quad q_4^2 = 0$$

The pion-pole contribution

- From the unitarity relation with only π^0 intermediate state, the pole residues in each channel are given by products of doubly-virtual and singly-virtual pion transition form factors ($\mathcal{F}_{\gamma^*\gamma^*\pi^0}$ and $\mathcal{F}_{\gamma^*\gamma\pi^0}$, input for our analysis)

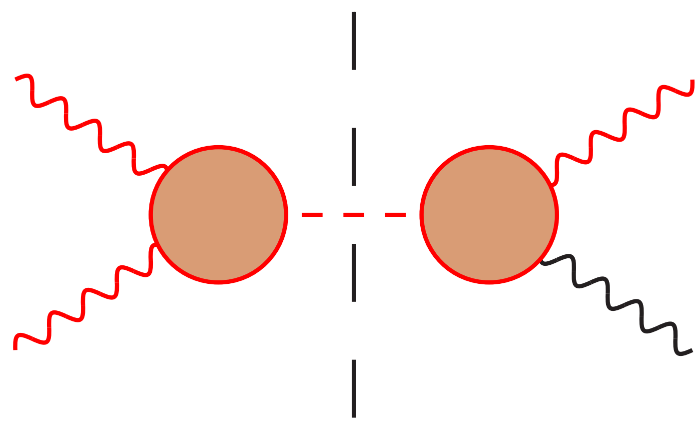

$$a_\mu^{\pi^0\text{-pole}} = \frac{2\alpha^3}{3\pi^2}\int_0^\infty dQ_1 \int_0^\infty dQ_2 \int_{-1}^1 d\tau \sqrt{1-\tau^2}\, Q_1^3 Q_2^3 \Big(T_1(Q_1,Q_2,\tau)\bar{\Pi}_1^{\pi^0\text{-pole}}(Q_1,Q_2,\tau) + T_2(Q_1,Q_2,\tau)\bar{\Pi}_2^{\pi^0\text{-pole}}(Q_1,Q_2,\tau)\Big)$$

with

$$\bar{\Pi}_1^{\pi^0\text{-pole}} = -\frac{\mathcal{F}_{\pi^0\gamma^*\gamma^*}(-Q_1^2,-Q_2^2)\mathcal{F}_{\pi^0\gamma^*\gamma^*}(-Q_3^2,0)}{Q_3^2+M_\pi^2} \qquad \bar{\Pi}_2^{\pi^0\text{-pole}} = -\frac{\mathcal{F}_{\pi^0\gamma^*\gamma^*}(-Q_1^2,-Q_3^2)\mathcal{F}_{\pi^0\gamma^*\gamma^*}(-Q_2^2,0)}{Q_2^2+M_\pi^2}$$

The pion-pole contribution

- From the unitarity relation with only π^0 intermediate state, the pole residues in each channel are given by products of doubly-virtual and singly-virtual pion transition form factors ($\mathcal{F}_{\gamma^*\gamma^*\pi^0}$ and $\mathcal{F}_{\gamma^*\gamma\pi^0}$, input for our analysis)

- These form factors can be reconstructed dispersively using
  - pion vector form factor
  - $\gamma^* \to 3\pi$ amplitude
  - elastic $\pi\pi$ scattering amplitude

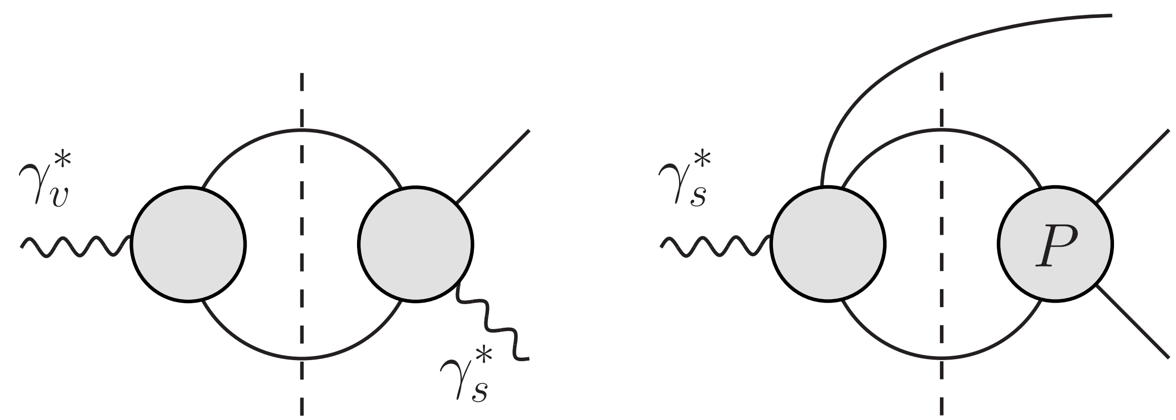

Hoferichter, Kubis, Leupold, Niecknig, Schneider (2014)

$\longrightarrow$ $$a_\mu^{\pi^0-\text{pole}} = 62.6^{+3.0}_{-2.5} \times 10^{-11}$$ Hoferichter, Hoid, Kubis, Leupold, Schneider (2018)

- Pseudoscalar poles with higher masses can be treated analogously

Pion-box contribution

- Defined by simultaneous two-pion cuts in two channels

- Contribution to scalar functions as dispersive integral of double spectral functions

$$\Pi_i = \frac{1}{\pi^2}\int ds'dt' \frac{\rho_i^{st}(s',t')}{(s'-s)(t'-t)} + (t \leftrightarrow u) + (s \leftrightarrow u)$$

- Dependence on q_i^2 carried by the pion vector FFs for each off-shell photon

- one-loop sQED projected onto the BTT structures fulfills the same Mandelstam representation of the pion box, the only difference being the pion vector FFs :

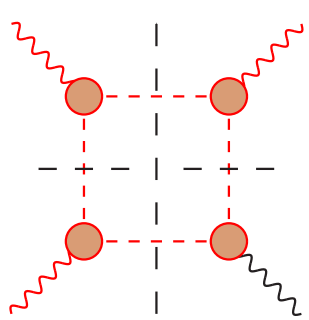

$$\equiv F_\pi^V(q_1^2)F_\pi^V(q_2^2)F_\pi^V(q_3^2)$$

$$\times \left[\qquad \right]$$

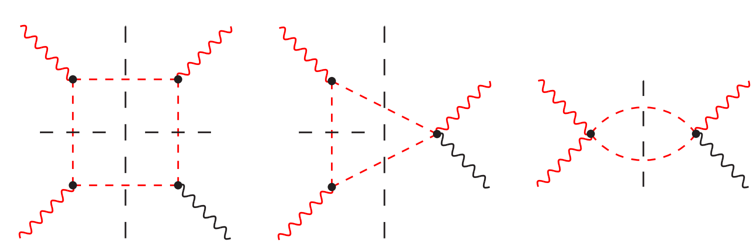

Numerics for the pion-box contribution

- The only input: pion vector form factor in the space-like region

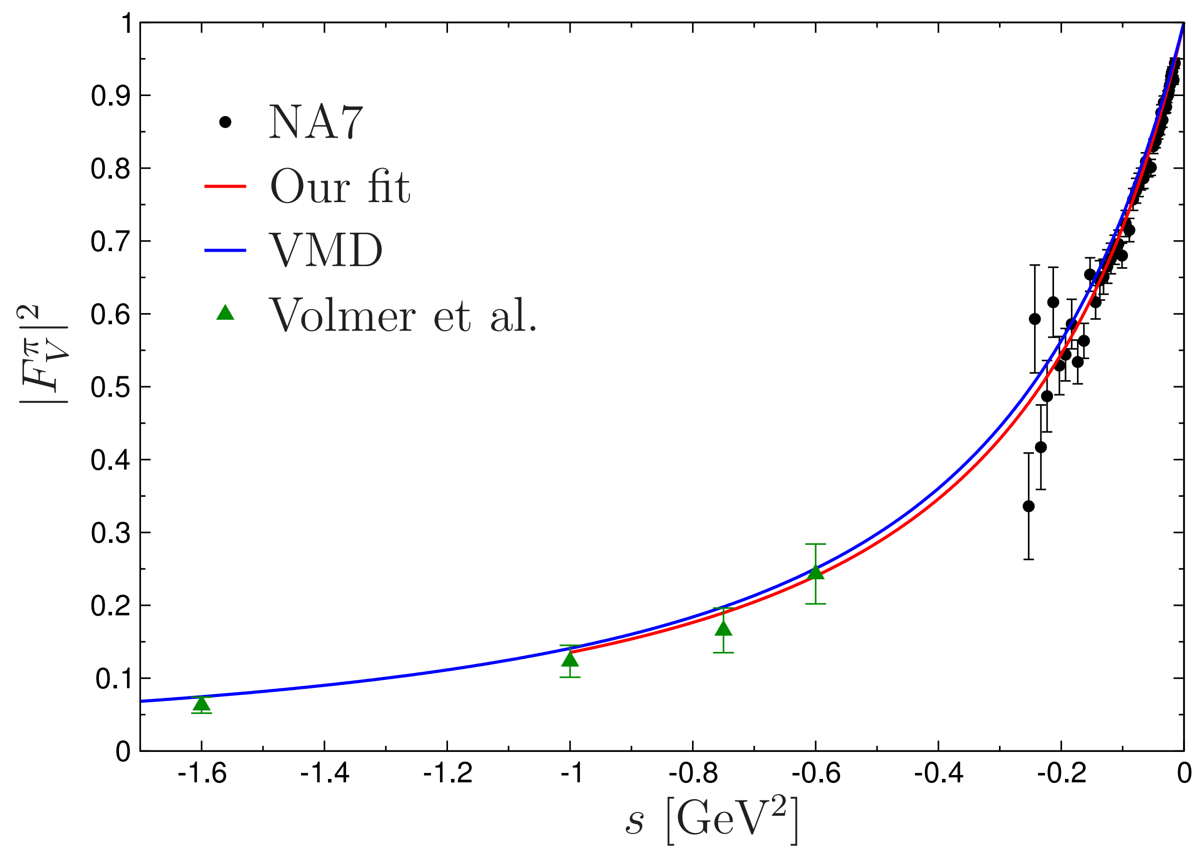

- Numerical results: $a_\mu^{\pi-\text{box}} = -15.9(2) \times 10^{-11}$ vs $a_\mu^{K-\text{box}\,,\text{VMD}} \simeq -0.5 \times 10^{-11}$

- Rapid convergence: $Q_{\text{max}} = \{1, 1.5\}$ GeV $\Rightarrow$ $a_\mu^{\pi\text{-box}} = \{95, 99\}\%$ of full result

The remaining ππ contribution

- Two-pion cut only in the direct channel: LH cut due to multi-particle intermediate states in the crossed channel neglected

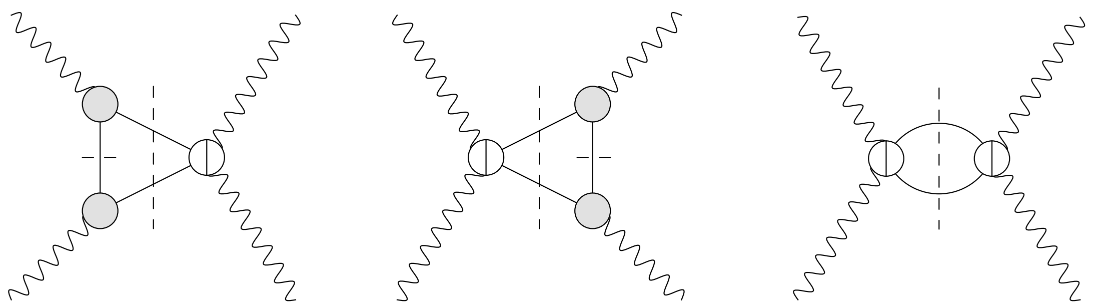

- Unitarity relates this contribution to the subprocess $\gamma^*\gamma^{(*)} \to \pi\pi$

- By generalizing previous analyses of $\gamma\gamma \to \pi\pi$ and $\gamma\gamma^* \to \pi\pi$ Moussallam et al. (2010, 2013) our goal is a dispersive reconstruction (based on analyticity, unitarity and crossing) of helicity partial waves for $\gamma^*\gamma^* \to \pi\pi$ Colangelo, Hoferichter, MP, Stoffer (2014)

- The solution of the resulting coupled set of dispersion relations involves elastic ππ phase shifts, which allows for the summation of ππ rescattering effects in the direct channel (effects of resonances coupling to ππ)

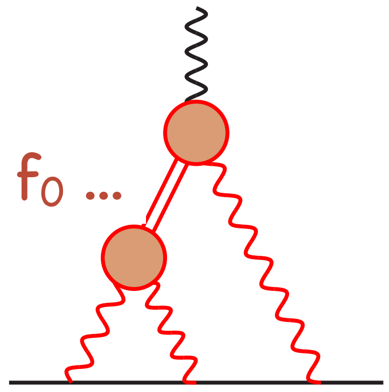

The remaining ππ contribution

- Contribution to a_μ^{HLbL} from $\gamma^*\gamma^* \to \pi\pi$ helicity partial waves :

$$\mathrm{Im}\, h^J_{++,++}(s; q_1^2, q_2^2; q_3^2, 0) = \frac{\sigma(s)}{16\pi} h^*_{J,++}(s; q_1^2, q_2^2)\, h_{J,++}(s; q_3^2, 0)$$

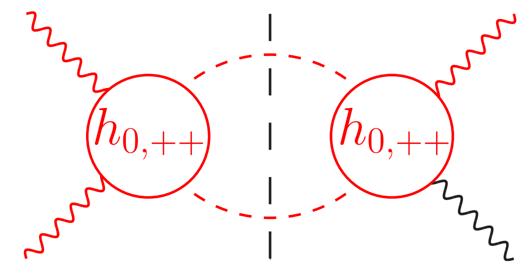

projecting onto BTT basis determines Im Π_i , from which Π_i for master formula.
Our framework holds for arbitrary partial waves.

- We solved dispersion relations for $\gamma^*\gamma^* \to \pi\pi$ S-waves taking:

  - pion pole as only LH singularity and phenomenological ππ phase shifts

a_μ^{HLbL} in 10^{-11} units

Λ	1 GeV	1.5 GeV	2 GeV	∞
$I = 0$	-9.2	-9.5	-9.3	-8.8
$I = 2$	2.0	1.3	1.1	0.9

$f_0(500)$ → $I = 0$

$$a_{\mu,J=0}^{\pi\pi,\pi\text{-pole LHC}} = -8(1) \times 10^{-11}$$